Thermodynamic Characterization of Radiant Coolers

Because of the performance sensitivity of radiant coolers to environmental conditions, orbits, configurations, and a wide range of heat loads and temperatures, it is difficult to establish a figure of merit or even compare the performance of different coolers, past and present. However, two parameters have been developed that allow a first-order comparison and a means to make preliminary estimates of cooler patch area requirements. First, the factors that go into the heat balance will be described; then, the derivation of the specific parameters will be discussed.

Radiant Cooler Heat Balance

The thermal heat balance equation for a single radiant cooler patch was given by Eqs. (5.1) and (5.2) in Chapter 5. Essentially, the same terms can be used in a slightly different way to achieve a different end. The overall heat balance for the cold patch is given by:

$$Q_{cp} = Q_c + Q_{\text{det}} + Q_{\text{par}}, \tag{6.1}$$

(6.1) Get MathML

where Q_{cp} is the total ideal heat rejection (cooling capacity) of the cold patch (in W), Q_c is the detector heater control power (W), Q_{det} is the detector electrical dissipation (W), and Q_{par} is the total parasitic (unwanted) heat load (W).

The total parasitic heat load on the cold patch comes from a number of sources. These have been combined into a single parameter to facilitate development of a new parameter later in this section. The total parasitic load is actually made up of the various specific loads:

$$Q_{\text{par}} = Q_{s/c} + Q_e + Q_o + Q_{sh} + Q_{\text{mli}} + Q_{\text{cond}} + Q_{ee}, \tag{6.2}$$

(6.2) Get MathML

where $Q_{s/c}$ is the energy emitted or reflected by spacecraft surfaces directly onto the cold patch; Q_e is Earth IR and albedo loads; Q_o is scene energy, i.e., radiation coming through optical elements and falling on the detectors or cold patch; Q_{sh} is the radiation from the cone shield, Earth shields, or other surfaces that have a view of the cold patch; Q_{mli} is the radiation through MLI blankets from warm surfaces around the patch or detectors; Q_{cond} is energy conducted via structural supports; and Q_{ee} is conduction via the electrical leads.

Performance Characterization and Comparison of Coolers

Rearrangement of some of the terms in Eq. (6.1) allows the development of a relatively simple method for characterizing cooler performance and comparing coolers. First the net cooling capability of a cooler (Q_{cp}) is defined by adding the detector dissipation and the heater power used for temperature control. Then (Q_{cp}) can be expressed by

$$Q_{cp} = Q_{\text{ideal}} - Q_{\text{par}}, \tag{6.3}$$

(6.3) Get MathML

where Q par is defined by Eq. (6.2) and Q_{ideal} is the ideal, or theoretical maximum, heat rejection of a cold patch (**W**), assuming a view factor of 100% to space; it can be expressed as

(6.4) $$Q_{\text{ideal}} = \sigma \varepsilon A T^4, \qquad (6.4)$$

Get MathML

where T is the temperature of the patch (K); ς is the Stefan-Boltzmann constant, 5.67×10^{-8} W/m^2·K^4; ε is the emittance of the cold patch surface (fin efficiency is assumed to be 100%); and A is the cold patch area (m^2).

The relative efficiency of a cooler can be measured by the fraction of the ideal cooling capacity that is taken up by parasitic loads. If the fraction of parasitics, f_p, is defined as

(6.5) $$f_p = Q_{\text{par}} / Q_{\text{ideal}}, \qquad (6.5)$$

Get MathML

then Eqs. (6.3) and (6.5) can be rearranged to yield an expression for f_p as a function of Q_{cp} and Q_{ideal}:

(6.6) $$f_p = 1 - Q_{cp} / Q_{\text{ideal}}. \qquad (6.6)$$

Get MathML

Substituting from Eq. (6.4) yields

(6.7) $$f_p = 1 - Q_{cp} / \sigma \varepsilon A T^4. \qquad (6.7)$$

Get MathML

Thus, knowing the net cooling capacity, cold patch area, emittance, and temperature, one can compute the value of f_p for any radiant cooler. Because the expression used for the ideal heat-rejection capacity assumes a view to space of 1.0 and a radiator fin efficiency of 1.0, and actual values achieved in the design will normally be less than 1.0, the deviations from ideal will also be reflected in the f_p value computed by Eq. (6.7). Another useful term can be derived by rearranging the elements of Eq. (6.7) to yield the area of the cold patch required per unit of cooling capacity for a given temperature, emittance, and f_p:

(6.8) $$\frac{A}{Q_{cp}} = \frac{1.76 \times 10^7}{\varepsilon T^4 (1 - f_p)}. \qquad (6.8)$$

Get MathML

Performances of radiant coolers are displayed for comparison in Fig. 6.13 using the parameters f_p and A/Q as a function of the cold-stage radiator temperature. Actual values used to generate the chart are shown in Table 6.5. For very small loads of a few milliwatts, the detector temperature is very close to the cold-stage radiator temperature. For larger loads, the detector may be typically 3–5 K higher than the cold-stage radiator. Separation of flight units, ground test units, and paper designs in Fig. 6.13, represented by differently shaded symbols, is defined by the legend on the chart. (Definitions for the acronyms used on the chart are found at the end of this chapter.)

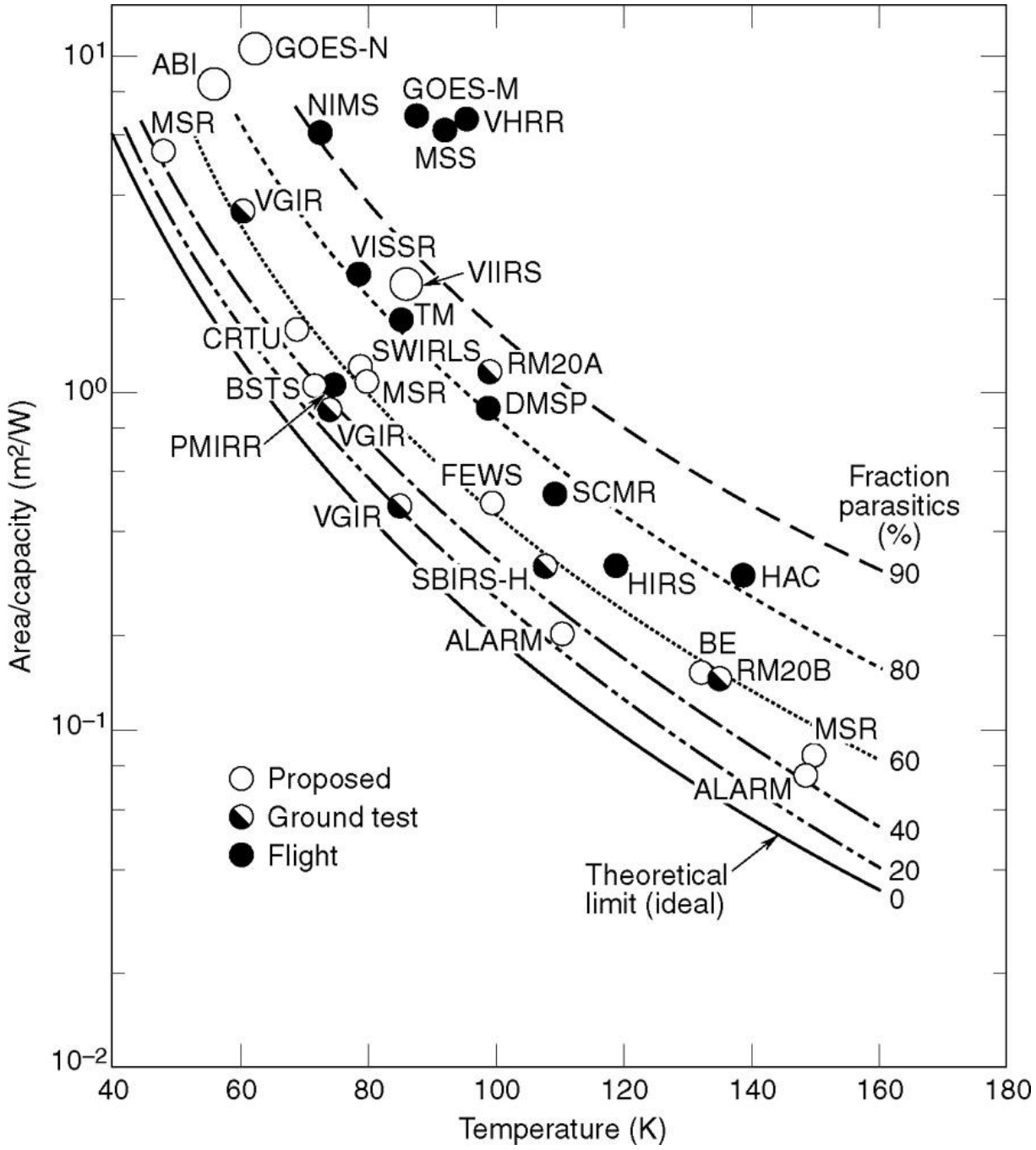

Figure 6.13: Performance of radiant coolers.

Table 6.5: Comparative Performance of Radiant Coolers

Radiator	Capacity (mW)	Temperature (K)	Fraction Parasitics (%)
BE	3400	133	57
CRTU	5000	70	55
DMSP	10	100	76

Table 6.5: Comparative Performance of Radiant Coolers

Radiator	**Capacity (mW)**	**Temperature (K)**	**Fraction Parasitics (%)**
FWS	5.8	175	84
HIRS	8	120	63
MSR	14,000	150	52
	915	80	61
	215	50	47
NIMS	10	75	91
PMIRR	39	75	47
RM20A	1000	100	84
RM20B	10,000	135	59
SCMR	5	110	68
SWIRLS	64	79	63
TM	26	87	81
VISSR	2	80	81
VHRR	1.5	97	97
VGIR	50	63	68
	400	85	27
FEWS	10,000	100	61
LLC	7000	195	—
Raytheon	1000	145	80
ALARM-1	2000	150	45
ALARM-2	3000	110	32

Table 6.5: Comparative Performance of Radiant Coolers

Radiator	Capacity (mW)	Temperature (K)	Fraction Parasitics (%)
BSTS	1720	72	35
ABI	125	60	53[a]
VIIRS	25	85	86
GOES-M	4	89	96
GOES-N[b]	2.5	65	91
SBIRS-H (GEO)	1500	110	57
ABI (modified)	125	60	68[c]

[a]Does not include support conduction.

[b]Estimated.

[c]Modified for support conduction.

Also shown on the chart are curves for constant values of f_p, in percent. In general, the efficiency of radiant coolers as measured by f_p becomes relatively poor as capacity and temperature are decreased. This chart can be used to provide broad guidelines in evaluation of proposed designs or predicting performance for various new applications. The bulk of the small-capacity-cooler data points fall between 80 and 90% parasitics; in other words, the FPA and control heater dissipation represents typically only 10 to 20% of the total cooling capacity of the cooler. For small-capacity coolers designed for GEO operation and using sun shields to accommodate solar loading at summer solstice (such as GOES I-M), parasitics can represent up to 95% of the total capacity. If these types of coolers can be mounted on spacecraft that perform yaw-flip maneuvers twice a year to preclude direct solar illumination, and radiant heat loads from spacecraft components such as solar sails, booms, and antennas are eliminated, then the parasitic fraction can probably be reduced to 60 or 70% of total capacity.

Data points shown for GOES I-M and GOES-N configurations in both Fig. 6.13 and Table 6.1 are calculated values, and their basis should be clarified. The values for GOES I-M are based on a cold patch area of 289 cm^2, a detector load of 4 mW with no heater operation, and a minimum patch temperature of 89 K. Values for GOES-N are merely predictions of what could be achieved if heat loads from solar sail and boom were eliminated and the cooler inverted during summer months.

Estimating Patch Area and Cooler Dimensions

A method for making preliminary estimates of the patch area and overall dimensions of a radiant cooler in geostationary orbit will be presented here in the form of a sample calculation. The following assumptions are made:

- There are no heat inputs from spacecraft protuberances such as masts, booms, sails, or antennas.
- Spacecraft yaw-flip maneuvers preclude direct solar impingement on the cooler.
- The radiant cooler has three stages:
    - The coldest (65 K) provides cooling for up to five FPA arrays, generating a heat load of 125 mW.
    - An intermediate stage (85 K) provides cooling for five FPA arrays, generating a heat load of 125 mW.
    - Another intermediate stage, at about 180 K, provides shielding for the lower-temperature stages and 20 W of cooling for the optics that operate at 210 K. (A temperature drop of 30 K is allowed for thermal margin and heat transport.)
- A temperature drop of 3 to 5 K is allowed between the radiators and the FPA arrays for the two coldest stages for margin, heater control, contamination, etc.
- The cooler housing temperature is controlled to 295 K.

The initial step in sizing the straw-man radiant cooler is to examine and review the data in Fig. 6.13 and several of the large coolers previously fabricated to provide an initial estimate of the 60 K cold patch area. Most of the coolers listed in Table 6.1 provide a single temperature level for FPA cooling (or in some cases two). When more than one FPA has been included, the patch area is based on the coldest temperature FPA. Use of multiple detectors and temperature levels will generally complicate the design and normally will lead to increased mass. Therefore, extrapolations to more complex designs from the data in Fig. 6.13 should be done very carefully; they will have limited accuracy.

Assuming a value of 65% for the percent parasitics and using Eq. (6.8), one can calculate an initial area of 0.51 m^2 for the 60 K panel. To determine the area and dimensions of the other stages, and to refine the 60 K panel area, a simple thermal model was constructed and a heat balance was conducted. Additional criteria and assumptions were made as follows:

- The emitting surfaces of each radiator stage were assumed to have an emittance of 0.95 based on a black-painted, open-cell honeycomb, such as those used on several radiant coolers and validated by the SBIRS-H configurations.
- Preliminary calculations indicated that a high-emittance radiator panel could absorb a peak of up to 300 mW/m^2 (orbit average of about 200 mW/m^2) of Earth IR and albedo without the use of shields. Therefore, highly specular shields were included to reject radiation approaching at an angle of less than 8.5 deg from parallel to the radiator. The inside of the shield was coated with VDA with a solar absorptance of 0.10 and IR emittance of 0.03.

Outside surfaces of the shields were assumed to be silver Teflon with solar absorptance of 0.20 and IR emittance of 0.78.

- Although detailed designs and analyses were beyond the scope of this sample effort, some preliminary allocations for heat transfer between the stages can be made based on a review of detail models of several past designs:
    - Structural support conductance of 0.0045 W/K is assumed.
    - Radiation through MLI blankets assumes an effective emittance of 0.01.
    - Conduction through wires and cables is assumed to be 0.001 W/K.

A simple geometric model was constructed and preliminary heat balances completed. The resulting area, temperatures, and dimensions are shown in Table 6.6. The resulting area for the 60 K stage is 0.54 m^2 and the overall dimension of the radiant cooler is estimated as 1.3 m. This is not an optimized cooler, but merely a straw-man design that appears feasible. Through the use of these data, two candidate concepts were generated. The configuration shown in Fig. 6.14(a) is defined as a coplanar type, and the configuration shown in Fig. 6.14(b) is defined as a SBIRS-H type, although a similar configuration (Fig. 6.4) was also built and tested by Rockwell International (now The Boeing Company) over 20 years ago.

Table 6.6: Characteristics of Radiant Cooler for Sample Problem

Stage	**Radiator Temperature (K)**	**Heat Load (mW)**	**Net Area Required (m2)**	**Gross Area Required (m2)**	**Dimensions for a Square Radiator (cm)**
3	60	125	0.541	0.541	73.6
2	82	125	0.624	1.16	108
1	184	20,000	0.372	1.53	124
Housing	295	—	—	1.61	127
Earth shields	206	—	—	—	130

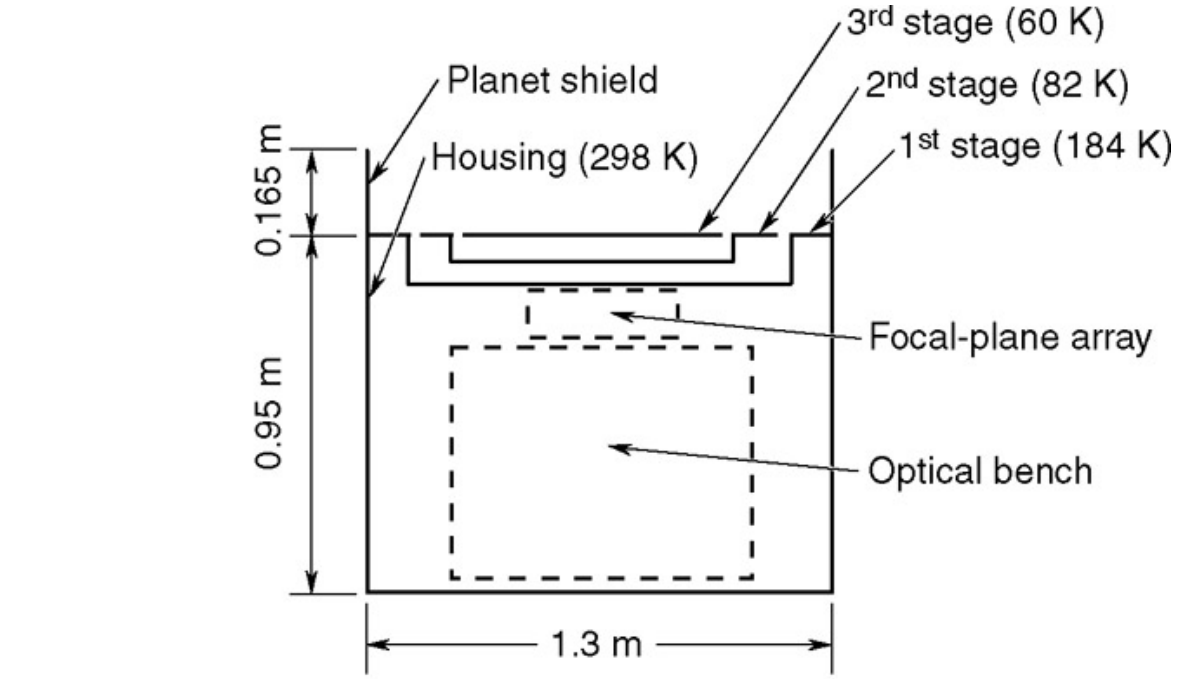

(a) Coplanar type

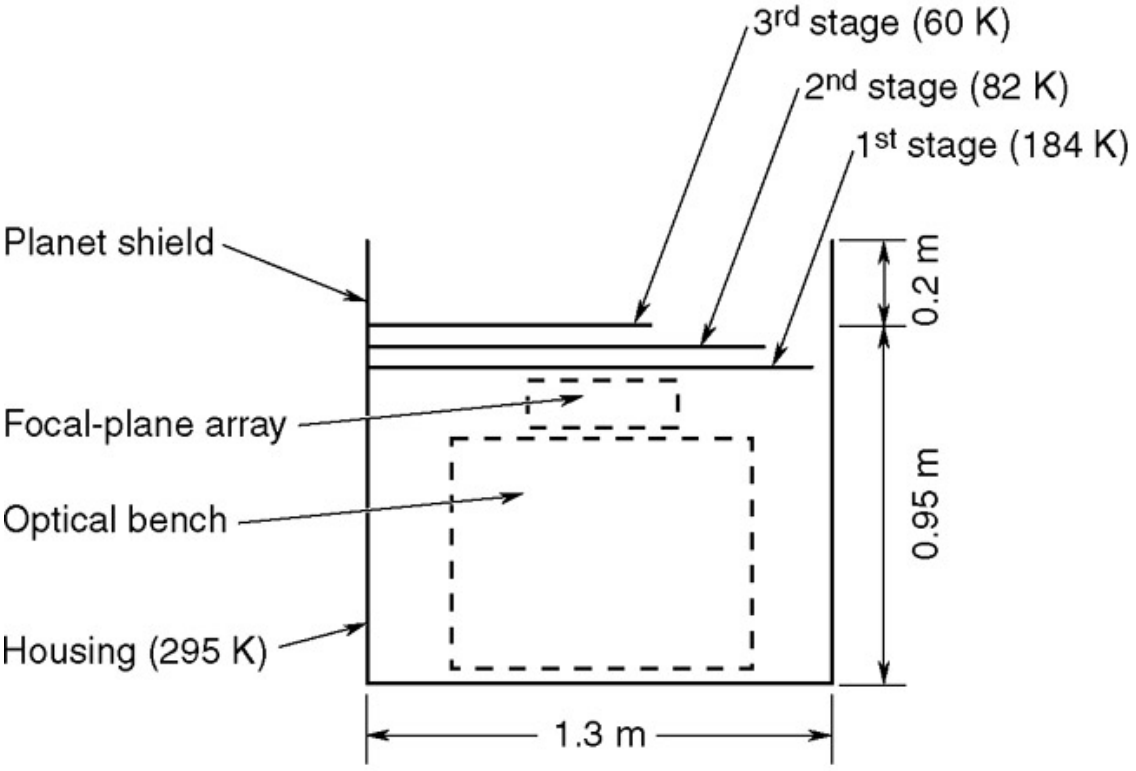

(b) SBIRS-H type

Figure 6.14: Cooler concepts for sample problem.

Preliminary analyses show that both of these concepts appear feasible and practical, based on the data available and the simplifying assumptions made. However, design, fabrication, and flight qualification of such a design would present significant technical challenges, depending on the weight and volume constraints placed on it.

Acronyms

ABI	Advanced Baseline Imager (Advanced GOES)
ACQ	Acquisition Sensor
ADL	A.D. Little
AEC	Able Engineering Company
AESD	Aerojet Electro-Optical Systems Division
ALARM	Alert, Locate and Report Missile
APR	Advanced Passive Radiator
AVHRR	Advanced Very High Resolution Radiometer
BAST	Ball Aerospace Systems and Technology
BE	Brilliant Eyes
BSTS	Boost Surveillance and Tracking System
CRTU	Cryogenic Radiator Test Unit
DSP	Defense Support Program
EMD	Engineering and Manufacturing Development
EOS	Earth Observing System
ERS-1	European Remote Sensing Satellite
ESA	European Space Agency
FEWS	Follow-On Early Warning System
FPA	Focal-Plane Assembly
FWS	Filter Wedge Spectrometer
GEO	Geosynchronous (or Geostationary) Earth Orbit
GOES	Geostationary Operational Environmental Satellite
GSFC	Goddard Space Flight Center

GVHRR	Geostationary Very High Resolution Radiometer
HAC	Hughes Aircraft Company (now Boeing Space Systems)
HIRS	High Resolution IR Sounder
HRIR	High Resolution IR Radiometer
HST	Hubble Space Telescope
ITT	International Telephone and Telegraph
JPL	Jet Propulsion Laboratory
LLC	Long Life Cooler
LM	Lockheed Martin
LMSC	Lockheed Missile and Space Company (now LM)
METSAT	Meteorological Satellite
MM	Martin Marietta (now LM)
MSG	Meteostat Second Generation
MSR	Multiple Stage Radiator
MSS	Multiple Spectral Scanner
NIMS	Near IR Mapping Spectrometer
NOAA	National Oceanic and Atmospheric Administration
NPOES	National Polar-Orbiting Operational Environmental Satellite
OLS	Operational Linescan System
PCM	Phase-Change Material
PMIRR	Pressure Modulator IR Radiometer
POES	Polar-Orbiting Operational Environmental Satellite
RCA	Radio Corporation of America
RI	Rockwell International (now The Boeing Company)
RM20	Radiometers for STP-72-2
RSC	Raytheon Systems Company
SBIRS-H	Space Based IR System-Hi

SBIRS-L Space Based IR System-Lo

SBRC Santa Barbara Research Center (Raytheon)

SCMR Surface Composition Mapping Radiometer

SEVIRI Spinning Enhanced Visible and IR Instrument

SSS Special Sensor-S

STP Space Test Program

SWIRLS Stratospheric Wind IR Limb Sounder

TM Thematic Mapper

TV Thermal Vacuum

USAF United States Air Force

VDA Vapor-Deposited Aluminum

VGIR V -Groove Isolation Radiator

VHRR Very High Resolution Radiometer

VIIRS Visual Integrated Imager Radiometer Suite

VISSR Visible Spin-Scan Radiometer

References

6.1 M. J. Donohoe and A. Sherman, "Radiant Coolers—Theory, Flight Histories, Design Comparison and Future Applications," AIAA Paper No. 75-184, 20 January 1975.

6.2 M. Donabedian, "Cryogenic Systems," Chap. 8 in *Satellite Thermal Control Handbook*, D. G. Gilmore, ed. (The Aerospace Press, El Segundo, CA, 1994).

6.3 M. Donabedian, "Cooling Systems," Chap. 15 in *The Infrared Handbook*, revised edition, W. L. Wolfe, ed. (Office of Naval Research, Washington, D.C., 1985).

6.4 T. T. Cafferty and D. J. Kuyper, "Radiative Cooler for the Thematic Mapper," *Proc. SPIE* **364** (10) (August 1982).

6.5 D. E. Wilson and J. P. Wright, "The Multistage Heat Pipe Radiator," AIAA Paper No. 77-760, June

1977.

6.6 J. P. Wright, "Development of a 5-watt, 70K Radiator," *AIAA 15th Thermophysics Conference* (10–14 July 1980).

6.7 *GOES I-M DataBook*, DRL-101-08, Rev. 1, 31 August 1996, prepared for NASA GSFC, Space Systems/Loral.

6.8 S. Bard, "Development of a High-Performance Cryogenic Radiator with V-Groove Radiation Shields," *J. Spacecraft and Rockets* **24** (3), 193 (May–June 1987).

6.9 C. Rasbach, "Thermal Design and Performance of a V-Groove Isolator Radiator," *AIAA, 26th Aerospace Science Meeting* (Reno, NV, 11–14 January1988).

6.10 Space Based Infrared System (SBIRS) technical brochure, Ball Aerospace and Technologies Corp., Aerospace Systems Division, Boulder, CO.

6.11 T. T. Cafferty, "Radiative Cryogenic Cooler for the Near IR Mapping Spectrometer for the GALILEO Jupiter Orbiter," Raytheon Company, Santa Barbara Research Center, Apri1 1981.

6.12 J. G. Ino and I. Wigbers, "The Design, Development and Qualification of the SCIAMACHY Radiant Cooler," Fokker Space B.V., The Netherlands, 25 July 1996.

6.13 D. D. Norris, JPL Task Plan 80-4867 Task 1 Report—Evaluating the Impact of Adding Infrared Bands to the Advanced Baseline Imager for GOES, JPL-D-18481, Jet Propulsion Laboratory, California Institute of Technology, November 1999.

6.14 H. Petersen and T. Wartel, "Passive Cryogenic Cooler for Meteosat SEVIRI Instrument," Paper # 67P., Fokker Space B.V., The Netherlands, 1996.

6.15 J. P. Wright and D. E. Wilson, "Fabrication of a 70K Heat Pipe Radiator," ASME Paper I No. 78-

ENAs-16, April1978.